Analysis and dynamics of measles with control strategies: a mathematical modeling approach

Olumuyiwa James Peter[1,2] · Hasan S. Panigoro[3] · Mahmoud A. Ibrahim[4,5] · Olusegun Michael Otunuga[6] · Tawakalt Abosede Ayoola[7] · Asimiyu Olalekan Oladapo[7]

Abstract

In this work, we examine the impact of certain preventive measures for effective measles control. To do this, a mathematical model for the dynamics of measles transmission is developed and analyzed. A suitable Lyapunov function is used to establish the global stability of the equilibrium points. Our analysis shows that the disease-free equilibrium is globally stable, with the measles dying out on the long run because the reproduction number $\mathcal{R}_0 \leq 1$. The condition for the global stability of the endemic equilibrium is also derived and analyzed. Our findings show that when $\mathcal{R}_0 > 1$, the endemic equilibrium is globally stable in the required feasible region. In this situation, measles will spread across the populace. A numerical simulation was performed to demonstrate and support the theoretical findings. The results suggest that lowering the effective contact with an infected person and increasing the rate of vaccinating susceptible people with high-efficacy vaccines will lower the prevalence of measles in the population.

✉ Olumuyiwa James Peter
  peterjames4real@gmail.com

1 Department of Mathematical and Computer Sciences, University of Medical Sciences, Ondo City, Ondo State, Nigeria

2 Department of Epidemiology and Biostatistics, School of Public Health, University of Medical Sciences, Ondo City, Ondo State, Nigeria

3 Biomathematics Research Group, Department of Mathematics, Faculty of Mathematics and Natural Sciences, State University of Gorontalo, Bone Bolango 96119, Indonesia

4 Bolyai Institute, University of Szeged, Aradi vértanúk tere 1., Szeged 6720, Hungary

5 Department of Mathematics, Faculty of Science, Mansoura University, Mansoura 35516, Egypt

6 Department of Mathematics, Augusta University, Augusta, GA, USA

7 Department of Mathematics, Osun State University, Osogbo, Nigeria

1 Introduction

Measles, also known as rubeola, is a viral infection that begins in the lungs. Despite the availability of a safe and efficient vaccination, it is still a leading cause of death globally. According to the World Health Organization, nearly 110,000 people died worldwide from measles in 2017, the majority of whom were children under the age of five [1]. Measles has an incubation period of about 8–12 days before the rash appears, followed by fever, cough, coryza, and conjunctivitis. Following these symptoms, a rash appears, which begins on the face and neck and spreads to the rest of the body [2]. The globe has had to deal with the measles pandemic on multiple occasions. Between 1988 and 1990, the United States of America experienced a measles outbreak, with over 16,000 cases and more than 70 deaths documented [3]. In 2018, Madagascar, Ukraine and Congo was hit by a measles outbreak that infected 50,000 individuals and claimed the lives of around 300 people, the majority of whom were children. Other countries like Angola, Cameroon, Kazakhstan, Chad, Nigeria, Thailand, Philippines, South Sudan, and Sudan are all experiencing the epidemics [4,5]. According to the 2013 Nigeria

Demographic and Health Survey, 25% of Nigerian children aged 12–23 months had got all recommended immunizations, whereas 42% had received measles vaccination. When compared to the Northern regions, the Southern regions had higher measles coverage (62–74%) (22–48%) [6]. The easiest way to avoid contracting measles is to be vaccinated. It's risk-free, cost-effective, and easy to use. Young children who have not been vaccinated and pregnant women are more vulnerable to measles and its complications, which can include death. Immunity against measles provided by vaccination has been proven to last for at least 20 years and is widely considered to be life-long for most people. At 9–11 months of age, the vaccine efficacy is estimated to be 85%, increasing to 97% following a second dose given at more than 12 months [7]. Children under the age of five and adults over the age of twenty are more likely to develop issues that necessitate hospitalization. Ear infections and diarrhea are two common complications. Pneumonia and encephalitis are serious consequences. Hospitalization is required in severe instances of measles. The Centers for Disease Control and Prevention (CDC) estimates that 1 in every 4 cases of measles in the United States results in hospitalization, and 1 in 1000 cases results in death, based on historical data. With widespread measles immunization, hospitalizations for measles dropped dramatically [8–10]. Mathematical models have become a significant tool that many researchers have utilized to better understand the epidemiology of diseases in various populations. To gain a better insight into the disease's transmission dynamics and control, many models have been developed and studied using various methodologies [11–19]. To understand the spread of measles, many scientists have employed mathematical models. Authors in [20] presented a basic SEIR model to examine the behavior of measles when no control is included in the model. The authors of [21] investigate the relationship between mass vaccination and herd immunity, whereas the authors of [22] consider the influence of vaccine on measles mortality in their model. The seasonality spreading factor was considered by the authors in [23] when discussing the transmission of measles in China. Furthermore, the authors in [24] consider early testing and therapy for those who have been exposed to measles in order to prevent subsequent outbreaks. Unlike the other references, the authors of [25] include passive immune groups in their model to investigate their impact on the measles eradication approach. The authors explain the impact of quarantine compartments in [2]. Few researchers have proposed a deterministic models by considering the transmission dynamics of the disease with double dose vaccination [5,7]. Other related studies on the dynamics of measles can be found in [26–29]. The current study aims to examine the impact of certain prevention measures, including vaccination and contact rate, for effective measles control. Our analysis will focus on the effectiveness of the first and second vaccination doses as well

as their coverage in preventing the spread of disease. Our inspiration came from a few research in the literature mentioned above that concentrated on deterministic modeling of measles; none of these studies looked at the impact of effective transmission rate, first dose vaccination rate, and second dose vaccination rate on the management of the disease. The rest of the paper is structured as follows: Sect. 2 deals with the formulation of the measles model and the model description. Section 3 deals with the equilibria and the basic reproduction number. Stability analysis and the numerical simulation are illustrated in Sects. 4 and 5, respectively, finally, the conclusion of the work is given in Sect. 6.

2 Formulation of the model

To study the dynamics of measles disease through a mathematical model approach, we divide the human population into seven classes, namely, susceptible class $S(t)$, individual who received the first dose of the MMR vaccine $V_1(t)$, individual who received the second dose of the MMR vaccine $V_2(t)$, exposed class $E(t)$, infected class $I(t)$, hospitalized class $H(t)$ and recovered class $R(t)$. Recruitment into the susceptible class is either by birth or immigration at the rate ϕ, susceptible individuals who received the first dose of vaccine moved to vaccinated compartment at a rate θ, due to the fact that the first dose of the MMR vaccine is not very effective to protect against measles, the first dose of vaccinated individuals can still be susceptible to the disease. In this case, the first dose of vaccinated individuals moves to the susceptible class at a rate β and those vaccinated with the first dose took the second dose at a rate σ_1. The second dose of vaccinated individuals moves to recovered class at a rate σ_2, susceptible individuals become exposed to the measles at the rate $\lambda = \alpha S I$, where α is the effective contact rate, the parameter ε represents the progression rate from exposed to infected class, while γ is the progression rate from infected class. Most people recovered from measles naturally without medication and in some cases, complications may occur whereby about one in five individuals infected will be hospitalized due to complications [30]. We have included hospitalized compartment in our model to illustrate this. It is assume that fraction ω recovers naturally while the rest moved to the hospitalized class. Upon treatment, individuals in the hospitalized class recovers at a rate τ, natural death rate occurs in all the compartments and it is assumed that death rate due to measles occurs only at the infected class at a rate δ. This description can be illustrated in the form of nonlinear differential equations and with the aid of schematic diagrams (see Fig. 1), our model takes the form:
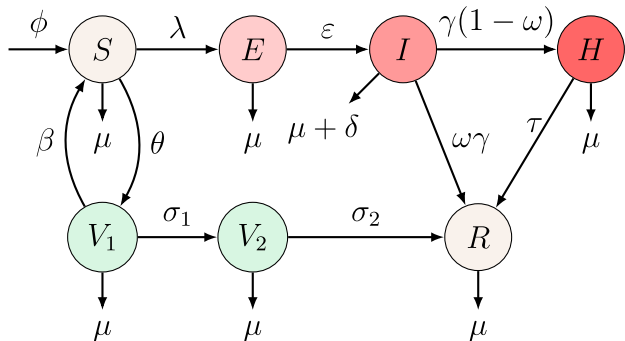
Fig. 1 Flowchart of model (1)

$$\frac{dS}{dt} = \phi - \alpha SI - (\theta + \mu)S + \beta V_1,$$

$$\frac{dV_1}{dt} = \theta S - (\beta + \mu + \sigma_1)V_1,$$

$$\frac{dV_2}{dt} = \sigma_1 V_1 - (\sigma_2 + \mu)V_2,$$

$$\frac{dE}{dt} = \alpha SI - (\varepsilon + \mu)E,$$

$$\frac{dI}{dt} = \varepsilon E - (\mu + \delta + \gamma)I,$$

$$\frac{dH}{dt} = \gamma(1 - \omega)I - (\mu + \tau)H,$$

$$\frac{dR}{dt} = \gamma \omega I + \tau H + \sigma_2 V_2 - \mu R,$$

(1)

where μ is is the natural death rate.

In case of no disease, for the total human population N with a positive initial condition

$$(S(0), V_1(0), V_2(0), E(0), I(0), H(0), R(0) \in R_+^7,$$

we have the equation

$$\frac{dN}{dt} = \phi - \mu N.$$

(2)

Equation (2) admits a unique equilibrium $N^* = \frac{\phi}{\mu}$ which is globally attractive on R_+.

3 Equilibria and the basic reproduction number

In this section, we show that system (1) has two equlibria dependent on the value of the basic reproduction number $\mathcal{R}_0$: the disease-free equilibrium E_0 if $\mathcal{R}_0 < 1$, and the endemic equilibrium E_1 when $\mathcal{R}_0 > 1$ (Table 1).

In the absence of the disease, we obtain the disease-free equilibrium of the system (1) by equating to zero the right side of equations in system (1). Hence, the disease-free equilibrium is given by

$$
\begin{aligned}
E_0 &= \left(S^*, V_1^*, V_2^*, E^*, I^*, H^*, R^*\right) \\
&= \left(\frac{\phi(\beta + \sigma_1 + \mu)}{\beta\mu + (\theta + \mu)(\sigma_1 + \mu)}, \frac{\theta\phi}{\beta\mu + (\theta + \mu)(\sigma_1 + \mu)}, \right. \\
&\quad \left. \frac{\theta\sigma_1\phi}{(\sigma_2 + \mu)(\beta\mu + (\theta + \mu)(\sigma_1 + \mu))}, 0, 0, 0, \frac{\sigma_2}{\mu}V_2^*\right),
\end{aligned}
$$

and always exists.

Next, we compute the basic reproduction number $\mathcal{R}_0$ of system (1), we follow the general approach established in [31]. Given the infectious states $E, I,$ and $H,$ and substituting the values of the disease-free equilibrium E_0, the matrices F and V are calculated for the new infection terms and the remaining transfer terms. . The matrices F and V are given as

$$
F = \begin{bmatrix} 0 & \alpha S^* & 0 \\ 0 & 0 & 0 \\ 0 & 0 & 0 \end{bmatrix} \text{ and } V = \begin{bmatrix} \varepsilon + \mu & 0 & 0 \\ -\varepsilon & \mu + \delta + \gamma & 0 \\ 0 & -\gamma(1 - \omega) & \mu + \tau \end{bmatrix}.
$$

(3)

The basic reproduction number, defined as the spectral radius of the matrix FV^{-1}, is given by

$$
\begin{aligned}
\mathcal{R}_0 &= \frac{\varepsilon\alpha S^*}{(\varepsilon + \mu)(\gamma + \delta + \mu)} \\
&= \frac{\varepsilon\alpha\phi(\beta + \sigma_1 + \mu)}{(\varepsilon + \mu)(\gamma + \delta + \mu)(\beta\mu + (\theta + \mu)(\sigma_1 + \mu))}.
\end{aligned}
$$

(4)

It is easy to prove that if $\mathcal{R}_0 > 1$, in addition to the disease-free equilibrium point E_0, system (1) also has an endemic equilibrium

$$E_1 = \left(S^{**}, V_1^{**}, V_2^{**}, E^{**}, I^{**}, H^{**}, R^{**}\right).$$

By solving the equations of the model in terms of the force of infection at steady state, we have that

$$S^{**} = \frac{(\varepsilon + \mu)(\delta + \gamma + \mu)}{\alpha\varepsilon},$$

$$V_1^{**} = \frac{\theta(\varepsilon + \mu)(\delta + \gamma + \mu)}{\alpha\varepsilon(\beta + \sigma_1 + \mu)},$$

$$V_2^{**} = \frac{\theta\sigma_1(\varepsilon + \mu)(\delta + \gamma + \mu)}{\alpha\varepsilon(\sigma_2 + \mu)(\beta + \sigma_1 + \mu)},$$

$$E^{**} = \frac{\phi}{\varepsilon + \mu}\left(1 - \frac{1}{\mathcal{R}_0}\right),$$

$$I^{**} = \frac{\varepsilon\phi}{(\varepsilon + \mu)(\delta + \gamma + \mu)}\left(1 - \frac{1}{\mathcal{R}_0}\right),$$

Table 1 Description of the models variables and parameters

Variable	Description
$S(t)$	Susceptible class
$V_1(t)$	People who received the first dose of the MMR vaccine
$V_2(t)$	People who received the second dose of the MMR vaccine
$E(t)$	Exposed class
$I(t)$	Infected class
$H(t)$	Hospitalized class
$R(t)$	Recovered class

Parameter	Description
ϕ	Recruitment rate of susceptible population
θ	First dose of vaccine rate
β	Movement rate from $V_1(t)$ to $S(t)$
σ_1	Second dose of vaccine rate
σ_2	Movement rate from $V_2(t)$ to $R(t)$
α	effective contact rate
ε	Progression rate from exposed to infected class
γ	Movement rate from infected class class
ω	Fraction of infected individuals who recovered naturally
$1 - \omega$	Fraction of infected individuals that are hospitalized
τ	Treatment rate of hospitalized individuals
μ	Natural death rate
δ	Measles induced death rate

$$H^{**} = \frac{\gamma(1-\omega)\varepsilon\phi}{(\tau+\mu)(\varepsilon+\mu)(\delta+\gamma+\mu)}\left(1 - \frac{1}{\mathcal{R}_0}\right)$$

$$R^{**} = \frac{\gamma\omega I^{**} + \tau H^{**} + \sigma_2 V_2^{**}}{\mu} \tag{5}$$

provided the basic reproduction number ($\mathcal{R}_0$) is greater than one. Since equation (1) is independent of the recovery population, we may concentrate our efforts on the following system:

$$\frac{dS}{dt} = \phi - \alpha SI - (\theta+\mu)S + \beta V_1,$$

$$\frac{dV_1}{dt} = \theta S - (\beta+\mu+\sigma_1)V_1,$$

$$\frac{dV_2}{dt} = \sigma_1 V_1 - (\sigma_2+\mu)V_2,$$

$$\frac{dE}{dt} = \alpha SI - (\varepsilon+\mu)E, \tag{6}$$

$$\frac{dI}{dt} = \varepsilon E - (\mu+\delta+\gamma)I,$$

$$\frac{dH}{dt} = \gamma(1-\omega)I - (\mu+\tau)H,$$

By the positivity and boundedness of the system solutions, we consider systems (1) and (6) in the positively invariant region

$$\Omega_1 = \Big\{ (S, V_1, V_2, E, I, H, R) \in \mathbb{R}^7 : \\ S + V_1 + V_2 + E + I + H + R \le \frac{\phi}{\mu} \Big\}, \tag{7}$$

and

$$\Omega = \Big\{ (S, V_1, V_2, E, I, H) \in \\ R^6 : S + V_1 + V_2 + E + I + H \le \frac{\phi}{\mu} \Big\}, \tag{8}$$

respectively.

4 Stability analysis

4.1 Local stability of the equilibrium points

In this section, we show the dynamics of our model depending on the basic reproduction number. We prove the local stability of the disease-free equilibrium E_0 of system (6) if the basic reproduction number $\mathcal{R}_0 < 1$, while if $\mathcal{R}_0 > 1$, then the endemic equilibrium E_1 is locally asymptotically stable.

Theorem 1 *The disease-free equilibrium E_0 is locally asymptotically stable if $\mathcal{R}_0 < 1$, and unstable otherwise.*

Proof The Jacobian matrix of the system (6) at E_0 is given by

$J(E_0)$

$$
= \begin{bmatrix}
-\theta - \mu & \beta & 0 & 0 & -\frac{\alpha\phi(\beta+\sigma_1+\mu)}{\beta\mu+(\theta+\mu)(\sigma_1+\mu)} & 0 \\
\theta & -\beta - \sigma_1 - \mu & 0 & 0 & 0 & 0 \\
0 & \sigma_1 & -\sigma_2 - \mu & 0 & 0 & 0 \\
0 & 0 & 0 & -\varepsilon - \mu & \frac{\alpha\phi(\beta+\sigma_1+\mu)}{\beta\mu+(\theta+\mu)(\sigma_1+\mu)} & 0 \\
0 & 0 & 0 & \varepsilon & -\delta - \gamma - \mu & 0 \\
0 & 0 & 0 & 0 & \gamma(1-\omega) & -\tau - \mu
\end{bmatrix}.
$$

It is easy to verify that two of the eigenvalues of $J(E_0)$ are $\lambda_1 = -\sigma_2 - \mu < 0$ and $\lambda_2 = -\tau - \mu < 0$. The remaining four eigenvalues can be obtained from the equation

$$
\begin{vmatrix}
-\theta - \mu - \lambda & \beta & 0 & -\frac{\alpha\phi(\beta+\sigma_1+\mu)}{\beta\mu+(\theta+\mu)(\sigma_1+\mu)} \\
\theta & -\beta - \sigma_1 - \mu - \lambda & 0 & 0 \\
0 & 0 & -\varepsilon - \mu - \lambda & \frac{\alpha\phi(\beta+\sigma_1+\mu)}{\beta\mu+(\theta+\mu)(\sigma_1+\mu)} \\
0 & 0 & \varepsilon & -\delta - \gamma - \mu - \lambda
\end{vmatrix} = 0,
$$

which gives the following characteristic equations:

$$
0 = \lambda^2 + (\beta + \sigma_1 + 2\mu + \theta)\lambda + (\beta + \sigma_1 + \mu)(\theta + \mu) - \beta\theta,
\tag{9}
$$

$$
0 = \lambda^2 + (\delta + \gamma + 2\mu + \varepsilon)\lambda + (\delta + \gamma + \mu)(\varepsilon + \mu) \\
- \frac{\varepsilon\alpha\phi(\beta + \sigma_1 + \mu)}{\beta\mu + (\theta + \mu)(\sigma_1 + \mu)}.
\tag{10}
$$

Equation (9) has two eigenvalues λ_3 and λ_4 as its roots satisfying the following:

$$
\lambda_3 + \lambda_4 = -\beta - \sigma_1 - 2\mu - \theta < 0, \\
\lambda_3\lambda_4 = (\beta + \sigma_1 + \mu)(\theta + \mu) - \beta\theta \\
= (\beta + \sigma_1 + \mu)\mu + (\sigma_1 + \mu)(\theta + \mu) > 0.
\tag{11}
$$

Again (10) has two eigenvalues λ_5 and λ_6 satisfying the following:

$$
\lambda_5 + \lambda_6 = -\delta - \gamma - 2\mu - \varepsilon < 0, \\
\lambda_5\lambda_6 = (\delta + \gamma + \mu)(\varepsilon + \mu)(1 - \mathcal{R}_0).
\tag{12}
$$

The conditions stated in (11) and (12) imply that $\lambda_3, \lambda_4, \lambda_5$, and λ_6 have negative real parts when $\mathcal{R}_0 < 1$. Therefore, E_0 is locally asymptotically stable if $\mathcal{R}_0 < 1$. If $\mathcal{R}_0 > 1$, at least one of λ_5 and λ_6 has a positive real part and E_0 is unstable. □

Theorem 2 *The endemic equilibrium E_1 is locally asymptotically stable if $\mathcal{R}_0 > 1$.*

Proof The Jacobian matrix of the system (6) at the endemic equilibrium E_1 is

$J(E_1)$

$$
= \begin{bmatrix}
-\alpha I^{**} - \theta - \mu & \beta & 0 & 0 & -\alpha S^{**} & 0 \\
\theta & -\beta - \sigma_1 - \mu & 0 & 0 & 0 & 0 \\
0 & \sigma_1 & -\sigma_2 - \mu & 0 & 0 & 0 \\
\alpha I^{**} & 0 & 0 & -\varepsilon - \mu & \alpha S^{**} & 0 \\
0 & 0 & 0 & \varepsilon & -\delta - \gamma - \mu & 0 \\
0 & 0 & 0 & 0 & \gamma(1-\omega) & -\tau - \mu
\end{bmatrix}.
$$

The Jacobian $J(E_1)$ has the following characteristic equation:

$$
(\lambda + \mu + \sigma_2)(\lambda + \mu + \tau)(\lambda^4 + C_3\lambda^3 + C_2\lambda^2 \\
+ C_1\lambda + C_0) = 0,
\tag{13}
$$

where

$$
\begin{aligned}
C_3 =& \alpha I^{**} + \beta + \delta + \varepsilon + \theta + \sigma_1 + \omega\gamma + 4\mu, \\
C_2 =& \alpha(\beta + \delta + \varepsilon + \sigma_1 + \omega\gamma + 3\mu)I^{**} \\
& + (\omega\gamma + \delta + \varepsilon)(\beta + \theta + \sigma_1 + 2\mu) + 3\mu(\beta + \theta + \sigma_1) \\
& + 5\mu^2 + \theta\sigma_1, \\
C_1 =& \alpha\left(2\mu(\beta + \varepsilon + \sigma_1) + (\beta + \varepsilon \right. \\
& + \sigma_1 + 2\mu)(\delta + \omega\gamma) + \varepsilon(\beta + \varepsilon + \sigma_1) + 3\mu^2\big)I^{**} \\
& + (\beta\mu + (\theta + \mu)(\sigma_1 + \mu))(\delta + \varepsilon + \gamma + 2\mu), \\
C_0 =& \alpha(\varepsilon + \mu)(\beta + \sigma_1 + \mu)(\delta + \gamma + \mu)I^{**}.
\end{aligned}
\tag{14}
$$

From (13), $J(E_1)$ has two negative eigenvalues are $-\mu - \sigma_1$ and $-\mu - \tau$. However, it is easy to verify from (14) that

$$
C_3 > 0,\ C_2 > 0,\ C_1 > 0,\ C_0 > 0 \text{ and } (C_3C_2 - C_1)C_1 \\
- C_3^2 C_0 > 0 \text{ if } I^{**} > 0.
$$

According to (5), $I^{**} > 0$ if $\mathcal{R}_0 > 1$, and hence, by Routh–Hurwitz stability criterion, the endemic equilibrium E_1 is locally asymptotically stable for $\mathcal{R}_0 > 1$. □

4.2 Global stability of the equilibrium points

Irrespective of where the system (1) starts, we wish to derive condition(s) under which the system converges to the disease-free E_0 or endemic equilibrium E_1 points on the long run. The following theorem shows condition for the global stability of the disease-free equilibrium E_0.

Theorem 3 *The disease-free equilibrium E_0 is globally stable in the feasible region Ω if $\mathcal{R}_0 \leq 1$.*

Proof Define the Lyapunov function $\mathcal{L} : \mathbb{R}_+^6 \to \mathbb{R}_+$ by

$$
\mathcal{L} = \left(S - S^* - S^* \ln \frac{S}{S^*}\right) \\
+ \sum_{j=1}^{2} r_j \left(V_j - V_j^* - V_j^* \ln \frac{V_j}{V_j^*}\right) \\
+ e_1 E + a_1 I + b_1 H,
\tag{15}
$$

where

$$e_1 = 1, \qquad (16)$$

$$r_1 = 1, \qquad (17)$$

$$a_1 = \frac{\varepsilon + \mu}{\varepsilon}, \qquad (18)$$

$$b_1 = \left(\frac{1}{\mathcal{R}_0} - 1\right)\frac{\alpha S^*}{(1-\omega)\gamma}, \qquad (19)$$

$$r_2 = \frac{\mu + \sigma_1}{\sigma_1}. \qquad (20)$$

It follows that

$$
\begin{aligned}
\frac{d\mathcal{L}}{dt} =\ & \phi + (\theta + \mu)S^* + r_1(\beta + \mu + \sigma_1)V_1^* \\
& + r_2(\mu + \sigma_2)V_2^* \\
& + \alpha(e_1 - 1)SI + (r_1\theta - \theta - \mu)S \\
& + (\beta + r_2\sigma_1 - r_1(\beta + \mu + \sigma_1))V_1 \\
& + I\left(\alpha S^* - a_1(\mu + \delta + \gamma) + b_1\gamma(1-\omega)\right) \\
& + (a_1\varepsilon - e_1(\mu + \varepsilon))E - \phi S^*/S - \beta S^* V_1/S \\
& - r_1\theta V_1^* S/V_1 - r_2(\mu + \sigma_2)V_2 - r_2\sigma_1 V_2^* V_1/V_2 \\
& - b_1(\mu + \tau)H.
\end{aligned}
\qquad (21)
$$

Define

$$\bar{s} = \frac{S}{S^*}, \quad \bar{v}_1 = \frac{V_1}{V_1^*}, \quad \bar{v}_2 = \frac{V_2}{V_2^*}, \qquad (22)$$

and

$$
\begin{aligned}
c_1 &= \mu S^*, \\
c_2 &= \beta V_1^*, \\
c_3 &= (\mu + \sigma_1)V_1^* = r_2(\mu + \sigma_2)V_2^*.
\end{aligned}
$$

It follows from (21) that

$$
\begin{aligned}
2c_1 + 2c_2 + 4c_3 =\ & \phi + (\theta + \mu)S^* + r_1(\beta + \mu + \sigma_1)V_1^* \\
& + r_2(\mu + \sigma_2)V_2^*,
\end{aligned}
$$

and

$$
\begin{aligned}
\frac{d\mathcal{L}}{dt} =\ & -c_1\left(\bar{s} + \frac{1}{\bar{s}} - 2\right) - c_2\left(\frac{\bar{v}_1}{\bar{s}} + \frac{\bar{s}}{\bar{v}_1} - 2\right) \\
& - c_3\left(\frac{\bar{v}_1}{\bar{v}_2} + \bar{v}_2 + \frac{\bar{s}}{\bar{v}_1} + \frac{1}{\bar{s}} - 4\right) - b_1(\mu + \tau)H.
\end{aligned}
\qquad (23)
$$

Using the fact that the arithmetic mean of a list of non-negative real numbers is greater than or equal to the geometric mean of the same list [32], it follows that $d\mathcal{L}/rmdt \le 0$. Equality holds if $S = S^*$, $V_k = V_k^*$ for $k = 1, 2$, $I = E = H = 0$. This implies that R converges to R^*. Since E_0 is the largest invariant set in the subset of Ω where $d\mathcal{L}/dt = 0$, its global stability follows by the LaSalle's Invariance Principle [33]. □

The following theorem shows condition for the global stability of the endemic equilibrium E_1.

Theorem 4 *The endemic equilibrium E_1 is globally stable in the feasible region Ω_1 if $\mathcal{R}_1 > 1$.*

Proof Assume $\mathcal{R}_0 > 1$. Then the existence of the endemic equilibrium E_1 given in (5) follows. Define the Lyapunov function $\mathbb{L} : \mathbb{R}_+^5 \to \mathbb{R}_+$ by

$$
\begin{aligned}
\mathbb{L} =\ & \left(S - S^{**} - S^{**}\ln\frac{S}{S^{**}}\right) \\
& + \sum_{j=1}^{2} \bar{r}_j\left(V_j - V_j^* - V_j^*\ln\frac{V_j}{V_j^*}\right) \\
& + \bar{e}_1\left(E - E^{**} - E^{**}\ln\frac{E}{E^{**}}\right) \qquad (24) \\
& + \bar{a}_1\left(I - I^{**} - I^{**}\ln\frac{I}{I^{**}}\right), \qquad (25)
\end{aligned}
$$

where

$$\bar{e}_1 = 1, \qquad (26)$$

$$\bar{r}_1 = 1, \qquad (27)$$

$$\bar{r}_2 = \frac{\mu + \sigma_1}{\sigma_1}, \qquad (28)$$

$$\bar{a}_1 = \frac{\varepsilon + \mu}{\varepsilon}. \qquad (29)$$

It follows that

$$
\begin{aligned}
\frac{d\mathbb{L}}{dt} =\ & \phi + (\theta + \mu)S^{**} + \bar{r}_1(\beta + \mu + \sigma_1)V_1^{**} \\
& + \bar{r}_2(\mu + \sigma_2)V_2^{**} \\
& + \bar{e}_1(\mu + \varepsilon)E^{**} + \bar{a}_1(\mu + \delta + \gamma)I^{**} \\
& + \alpha(\bar{e}_1 - 1)SI + (\bar{r}_1\theta - \theta - \mu)S \\
& + (\beta + \bar{r}_2\sigma_1 - \bar{r}_1(\beta + \mu + \sigma_1))V_1 \\
& + I\left(\alpha S^{**} - \bar{a}_1(\mu + \delta + \gamma)\right) + (\bar{a}_1\varepsilon - \bar{e}_1(\mu + \varepsilon))E \\
& - \phi S^{**}/S - \beta S^{**}V_1/S \\
& - \bar{r}_1\theta V_1^{**}S/V_1 - \bar{r}_2(\mu + \sigma_2)V_2 \\
& - \bar{r}_2\sigma_1 V_2^{**}V_1/V_2 - \bar{e}_1\alpha E^{**}SI/E - \bar{a}_1\varepsilon I^{**}E/I.
\end{aligned}
\qquad (30)
$$

Define

$$\hat{s} = \frac{S}{S^{**}}, \quad \hat{v}_1 = \frac{V_1}{V_1^{**}}, \quad \hat{v}_2 = \frac{V_2}{V_2^{**}}, \quad \hat{e} = \frac{E}{E^{**}}, \quad \hat{i} = \frac{I}{I^{**}}.$$

and

$$\bar{c}_1 = \mu S^{**}, \qquad (31)$$

$$\bar{c}_2 = \beta V_1^{**}, \qquad (32)$$

$$\bar{c}_3 = \bar{r}_2\sigma_1 V_1^{**} = \bar{r}_2(\mu + \sigma_2)V_2^{**}, \tag{33}$$

$$\bar{c}_4 = \bar{e}_1\alpha S^{**}I^{**} = \bar{a}_1\varepsilon E^{**}. \tag{34}$$

It follows from (30) that

$$
\begin{aligned}
2\bar{c}_1 + 2\bar{c}_2 + 4\bar{c}_3 + 3\bar{c}_4 + = {}& \phi + (\theta + \mu)S^{**} \\
& + \bar{r}_1(\beta + \mu + \sigma_1)V_1^{**} \\
& + \bar{r}_2(\mu + \sigma_2)V_2^{**} \\
& + \bar{e}_1(\mu + \varepsilon)E^{**} \\
& + \bar{a}_1(\mu + \delta + \gamma)I^{**},
\end{aligned}
\tag{35}
$$

and

$$
\begin{aligned}
\frac{d\mathbb{L}}{dt} = {}& -\bar{c}_1\left(\hat{s} + \frac{1}{\hat{s}} - 2\right) \\
& -\bar{c}_2\left(\frac{\hat{v}_1}{\hat{s}} + \frac{\hat{s}}{\hat{v}_1} - 2\right) \\
& -\bar{c}_3\left(\frac{\hat{v}_1}{\hat{v}_2} + \hat{v}_2 + \frac{\hat{s}}{\hat{v}_1} + \frac{1}{\hat{s}} - 4\right) \\
& -\bar{c}_4\left(\frac{\hat{s}\hat{i}}{\hat{e}} + \frac{\hat{e}}{\hat{i}} + \frac{1}{\hat{s}} - 3\right).
\end{aligned}
\tag{36}
$$

Using the fact that the arithmetic mean of a list of non-negative real numbers is greater than or equal to the geometric mean of the same list [32], it follows that $d\mathbb{L}/dt \leq 0$. Equality holds if $S = S^{**}$, $V_k = V_k^{**}$ for $k = 1, 2$, $I = I^{**}$, $E = E^{**}$. This implies that H converges to H^{**} and R converges to R^*. Since E_1 is the largest invariant set in the subset of Ω where $d\mathbb{L}/dt = 0$, its global stability follows by the LaSalle's Invariance Principle [33]. □

5 Numerical simulations

5.1 Parameter values

Some of the parameter values used in the simulation process are published parameters obtained from the literature. Those not found in the literature are estimated. Parameters based on the Nigeria data on measles for the year 2020 are obtained from [34] (Fig. 3).

Using the estimated and published parameters given in Table 2, the system (1) converges to the disease-free equilibrium E_0 irrespective of the initial condition used, and the reproduction number $\mathcal{R}_0 < 1$. The population receiving the first and second doses of the MMR converge to 73,083 and 84,926, respectively. The susceptible and the recovered class converge to 118,979 and 219,875,114, respectively, while the infected classes converge to zero. This analysis shows that the effect of the vaccines is significant, with the second

dose of the vaccine having more effect than the first dose. The numerical simulations of these conditions are given in Fig. 2. Now, to show the influence of the interaction between the susceptible and infected classes, we increase the value of the impact of the contact rate to $\alpha = 1 \times 10^{-5}$. The reproduction number increases such that $\mathcal{R}_0 > 1$ which means E_1 becomes asymptotically stable and measles exists in the population. As the contact rate increases, the susceptible class, people who received the first dose of the MMR vaccine, people who received the second dose of the MMR vaccine, and the recovered class will decrease to 46,632, 28,644, 33,286, and 209,908,515, respectively. Measles becomes endemic which is indicated by the occurrence of exposed, infected, and hospitalized classes which, respectively, converge to 82,679, 88,706, and 55,940. Here, we can say that restricting the interaction between susceptible and infected classes play the important role in suppressing the growth rate of exposed and infected class. To learn more about the most influential parameter to the infection rate and the density for each class, the global sensitivity analysis is given in the following sub-section.

5.2 Global sensitivity analysis

To investigate the most influential parameter in model (1), the global sensitivity analysis is employed. Two biological aspects namely the basic reproduction number and the density of each class become the constraint functions of the sensitivity analysis while the ranks of the parameters are the objective function. To facilitate these works, the Partial Rank Correlation (PRCC) [35] is used for ranking along with Saltelli sampling [36,37] to generate more than 2000 sample data around the parameter values given in Table 2. The values of ψ and μ are fixed by considering the estimated parameters based on the data. Therefore, the parameters $\theta, \delta, \gamma, \sigma_1, \beta, \alpha$, and ε will be ranked while σ_2, ω and τ are also fixed since these two parameters do not affect the value of $\mathcal{R}_0$. The PRCC results lie on $-1 < \mathcal{P} < 1$ where $\mathcal{P}$ is set of parameter values. The most sensitive parameter given is derived using the greatest value of $|\mathcal{P}|$. The sign of $\mathcal{P}$ indicates the relationship between the parameter with the values of the constraint functions in these cases being the reproduction number and the density of each class.

We first analyze the global sensitivity of parameters to the reproduction number ($\mathcal{R}_0$) and achieved that α as the effective contact rate becomes the most influential parameter with PRCC value is 0.88 as given by Fig. 4. This means that the policy-making on controlling the effective contact rate plays a major part in the existence of measles. By observing the sign of PRCC, we also know that the contact rate is directly proportional to the increase of reproduction number. The next ranks are, respectively, occupied by $\gamma, \theta, \beta, \sigma_1, \delta$, and ε, where β has positive relationship with $\mathcal{R}_0$ while others
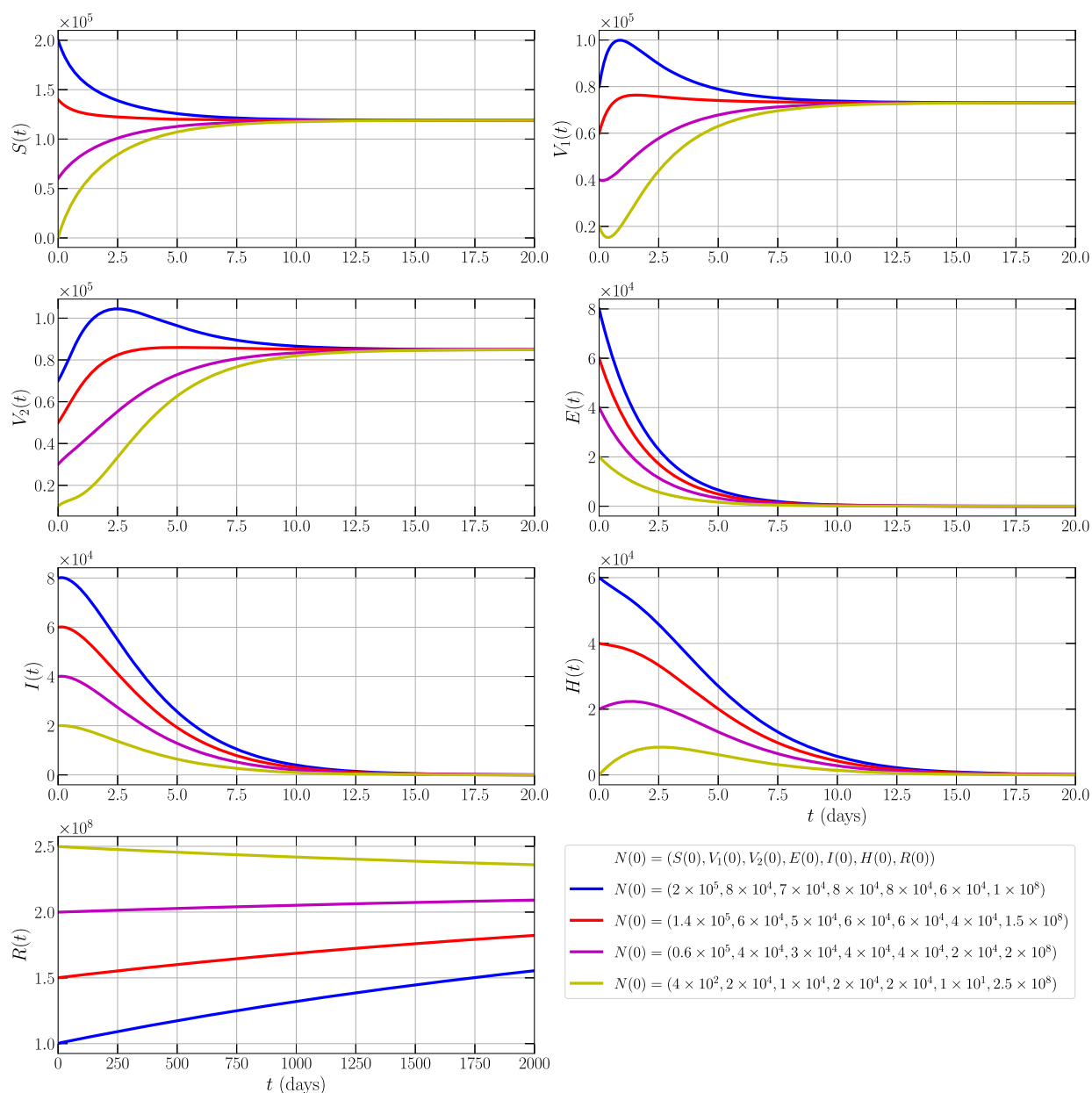
Fig. 2 Time series of model (1) using parameters given by Table 2

have negative relationship. This means that by increasing the movement rate from V_1 to S, the reproduction number also increases. While increasing the movement rate from infected class, the first dose vaccine rate, the second dose vaccine, the measles death rate, and the progression rate from exposed to infected class, the basic reproduction number will decrease. We show all of these biological conditions in some contour plots given by Fig. 5.

Now, the global sensitivity analysis of parameters with respect to the density for each class is investigated. The numerical process is given as follows. We first generate random data using Saltelli sampling and compute the numerical

solutions using 4th-order Runge-Kutta method. The PRCC results are given in Fig. 6. The most influential parameter is decided by observing the convergence of PRCC when time moves forward. As a result, we have the most influential parameter for each class given in Table 3. The most influential parameter for both people who received the first and second dose of the MMR vaccine ($V_1(t)$ and $V_2(t)$) is given by the second dose of vaccine rate (σ_1) (where the PRCC results are -0.99994 and 0.64932), respectively. The PRCC results show that σ_1 has negative relationship with $V_1(t)$ and positive relationship with $V_2(t)$ which means that by increasing the second dose vaccine rate, the number of peo-
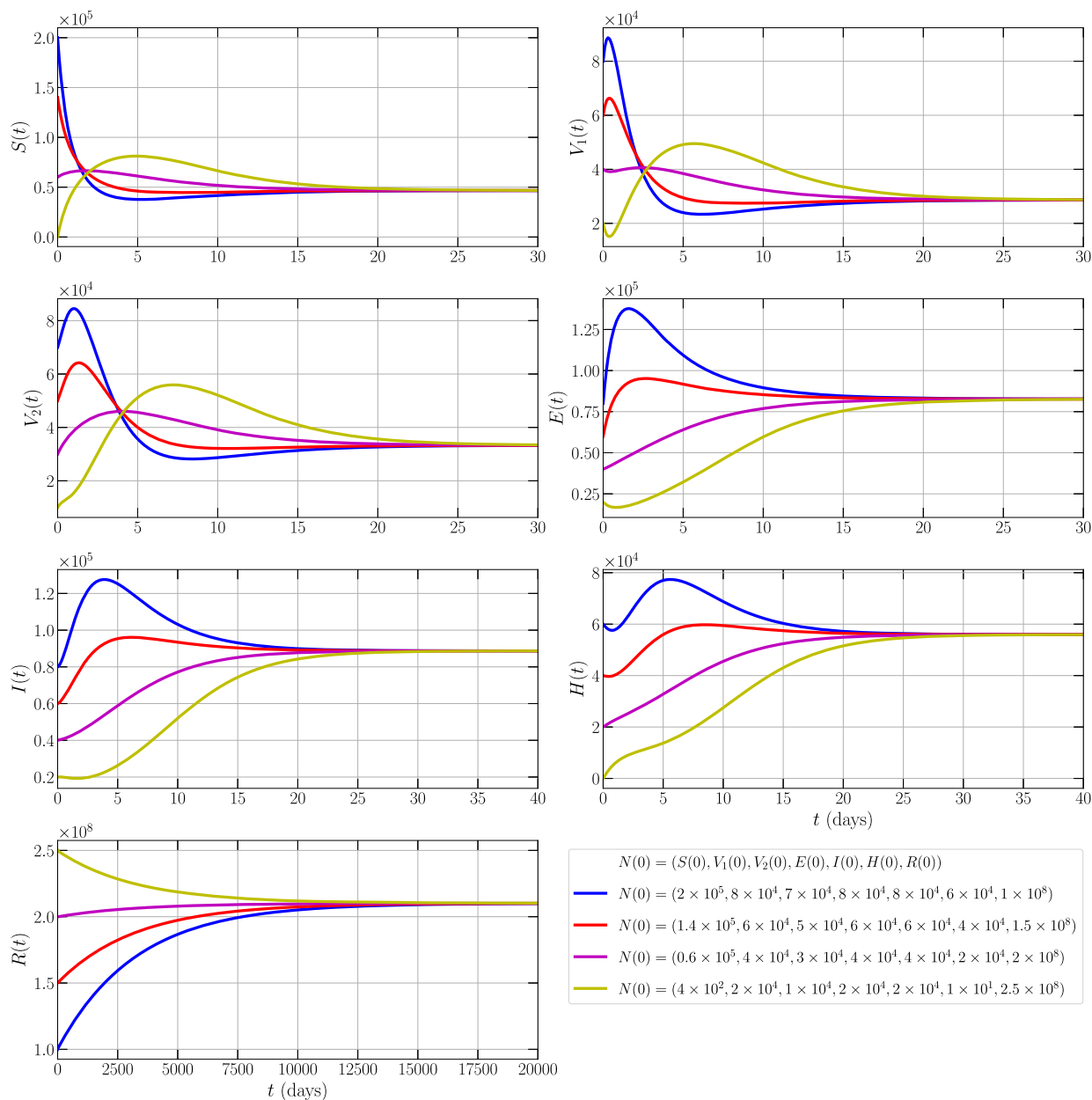
Fig. 3 Time series of model (1) using parameters given by Table 2

Table 3 The most influential parameter for each class observes by PRCC

Variable	Most influential parameter	PRCC result
V_1	σ_1	-0.99994
V_2	σ_1	0.64932
E	α	0.84982
I	γ	-0.92559
H	δ	-0.44630
R	θ	0.67734

ple who only receive the first dose will decrease while those receiving the second dose will increase. For the exposed class ($E(t)$), the PRCC results show that the effective contact rate (α) becomes the most influential parameter in increasing its density. We also successfully compute the PRCC results for infected class ($I(t)$), hospitalized class ($H(t)$), and recovered class ($R(t)$). The sign of PRCC values indicate that movement rate from infected class and measles death rate have negative relationship with the densities of infected and hospitalized class while the first dose of vaccine rate has positive relationship with recovered class.

Fig. 4 PRCC results for the parameters of $\mathcal{R}_0$
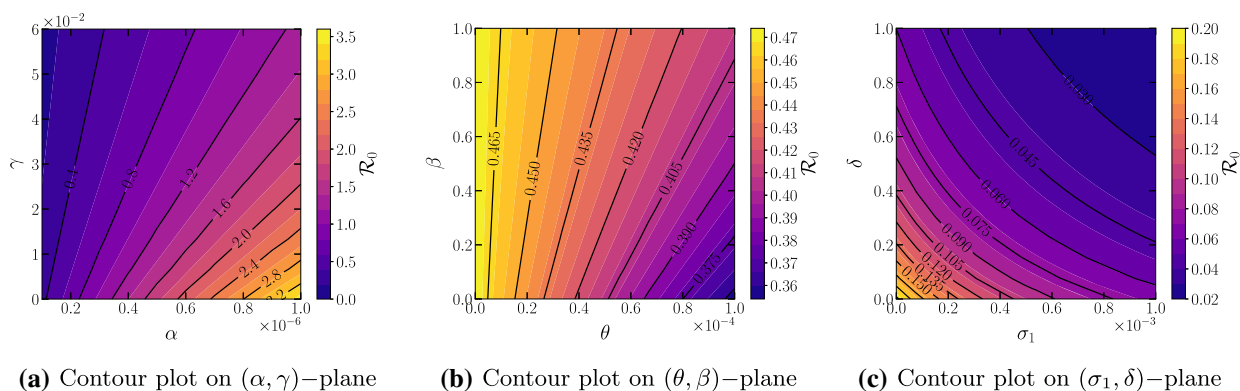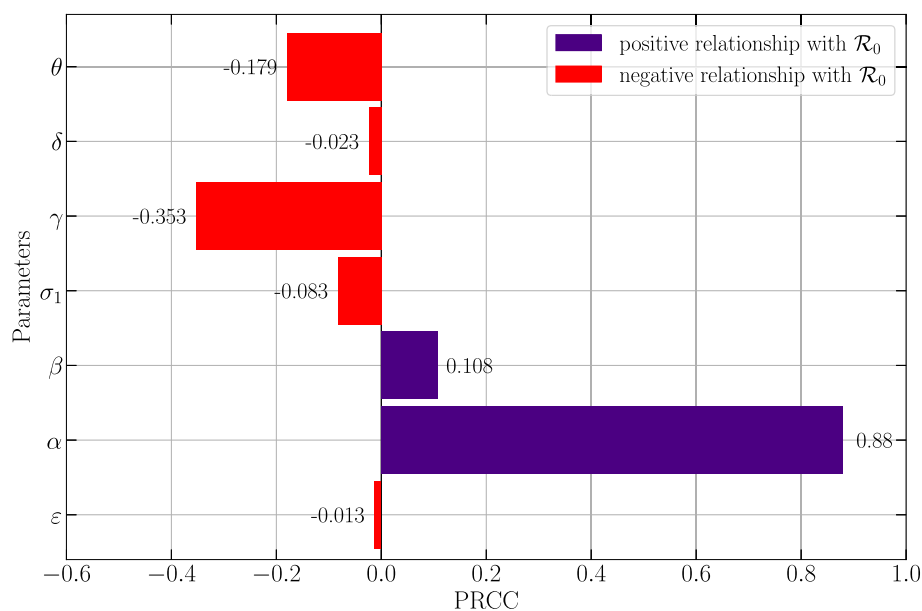
Fig. 5 Contour plots for the parameters respect to $\mathcal{R}_0$

(a) Contour plot on $(\alpha, \gamma)-$plane   **(b)** Contour plot on $(\theta, \beta)-$plane   **(c)** Contour plot on $(\sigma_1, \delta)-$plane

Table 2 The description of parameters and values

Parameter	Description	Value	Source
ϕ	Recruitment rate into susceptible class	68027	Estimated
μ	Natural death rate	0.000309	Estimated
δ	Measles death rate	0.033720	Estimated
θ	First dose of vaccine rate	0.94	[1]
β	Movement rate from $V_1(t)$ to $S(t)$	0.6	[2]
σ_1	Second dose of vaccine rate	0.93	[1]
σ_2	Movement rate from $V_2(t)$ to $R(t)$	0.8	[2]
α	effective contact rate	1×10^{-9}	Fitted
ε	Progression rate from exposed to infected class	0.500000	Estimated
γ	Movement rate from infected class	0.432	Fitted from [34]
ω	Fraction of infected individuals who recovered naturally	0.062366	Fitted from [34]
τ	Treatment rate of hospitalized individuals	0.642	Fitted from [34]
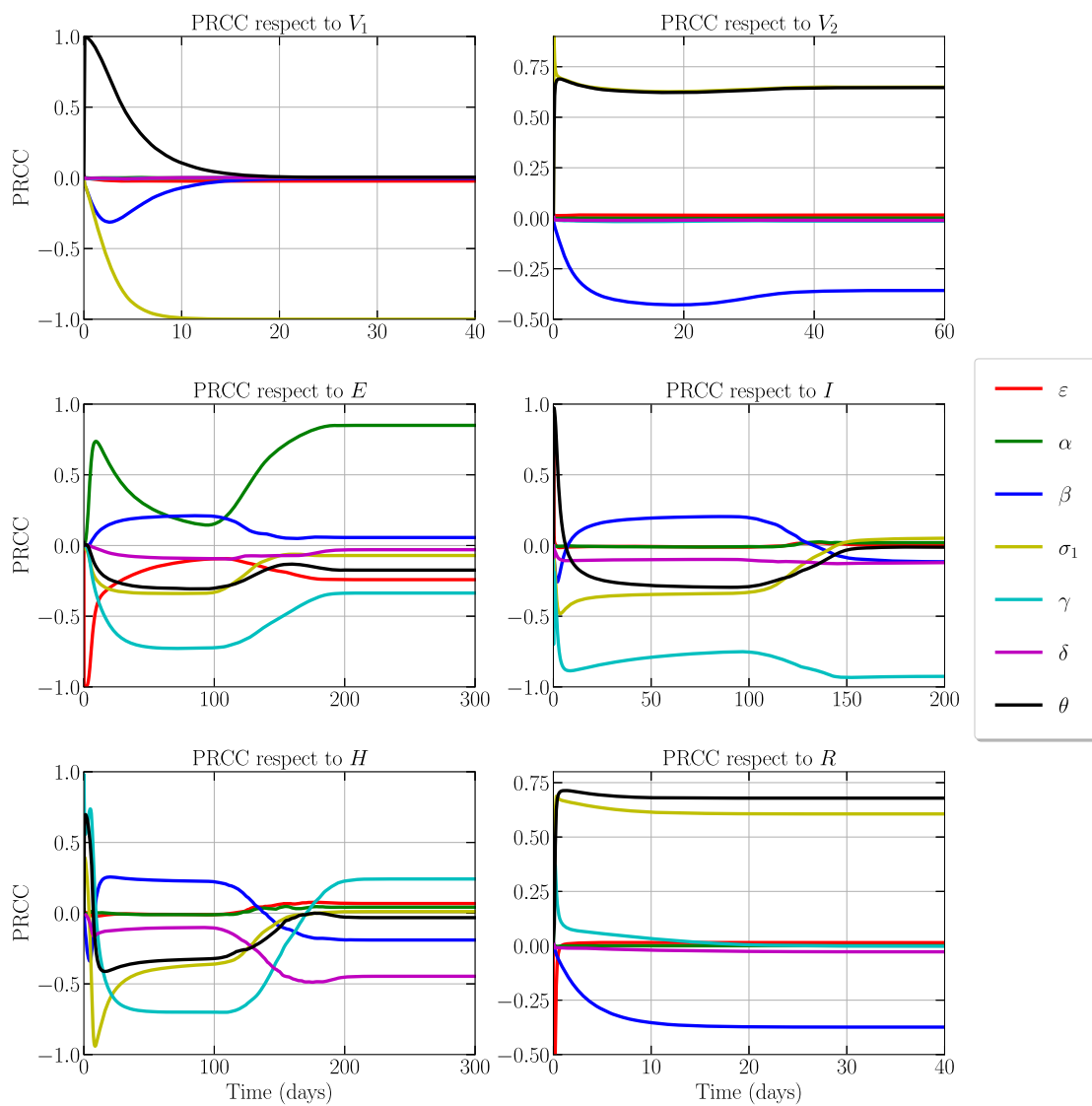
Fig. 6 PRCC results for the parameters of V_1, V_2, E, I, H, and R
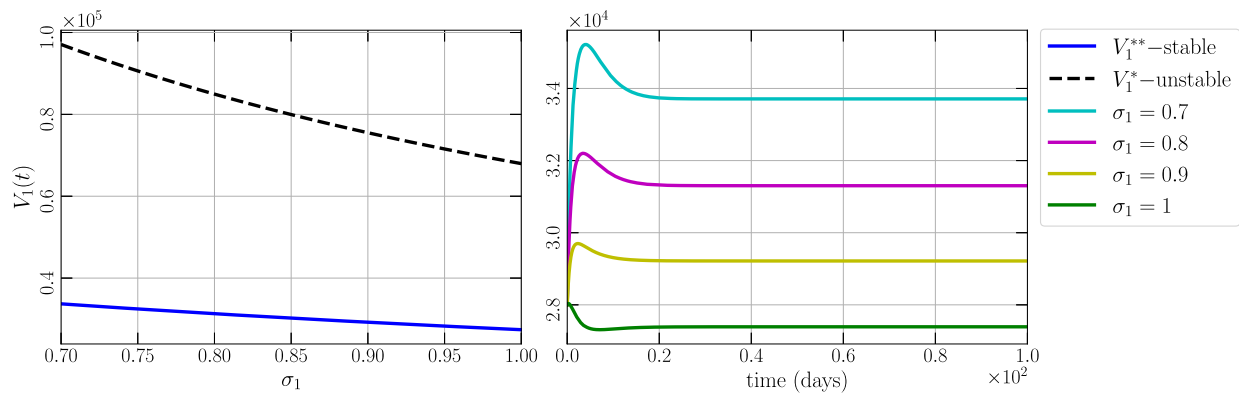
Fig. 7 Bifurcation diagram driven by σ_1 and time-series of model (1) respect to $V_1(t)$
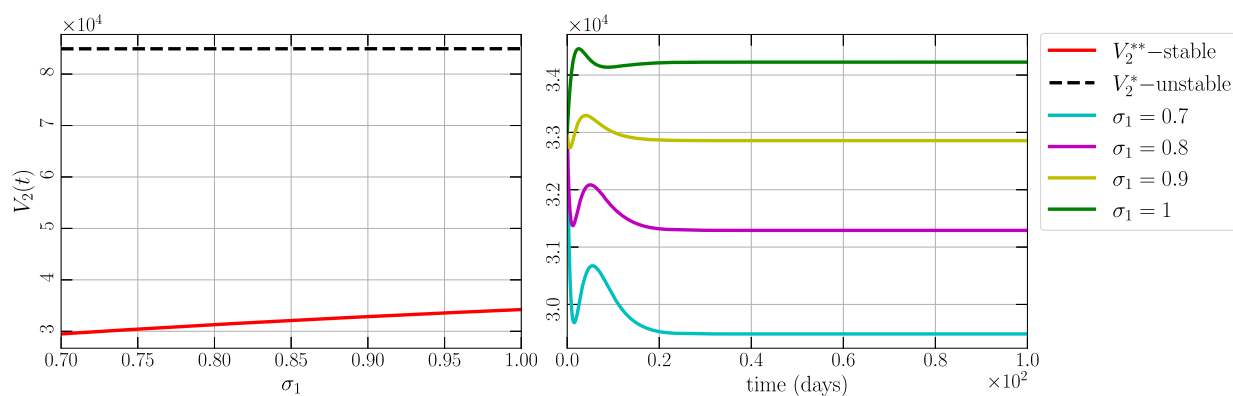
Fig. 8 Bifurcation diagram driven by σ_1 and time-series of model (1) respect to $V_2(t)$
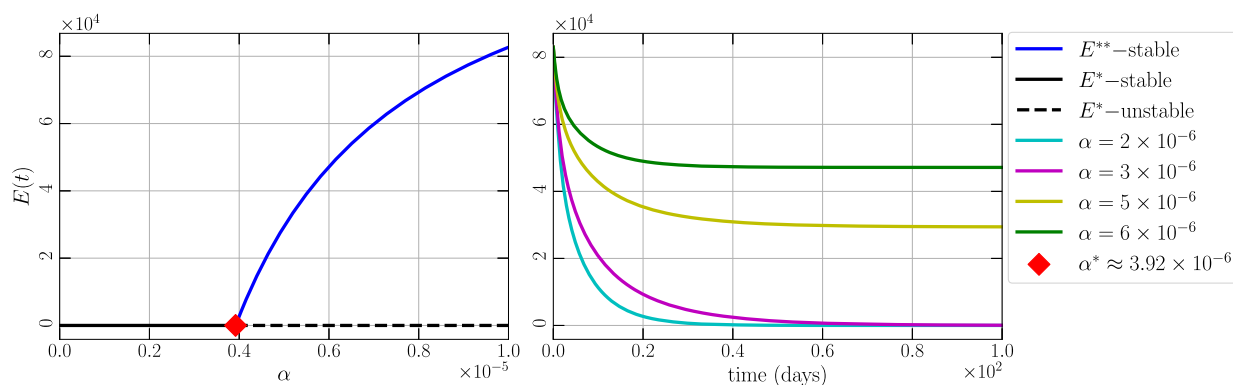
Fig. 9 Bifurcation diagram driven by α and time-series of model (1) respect to $E(t)$
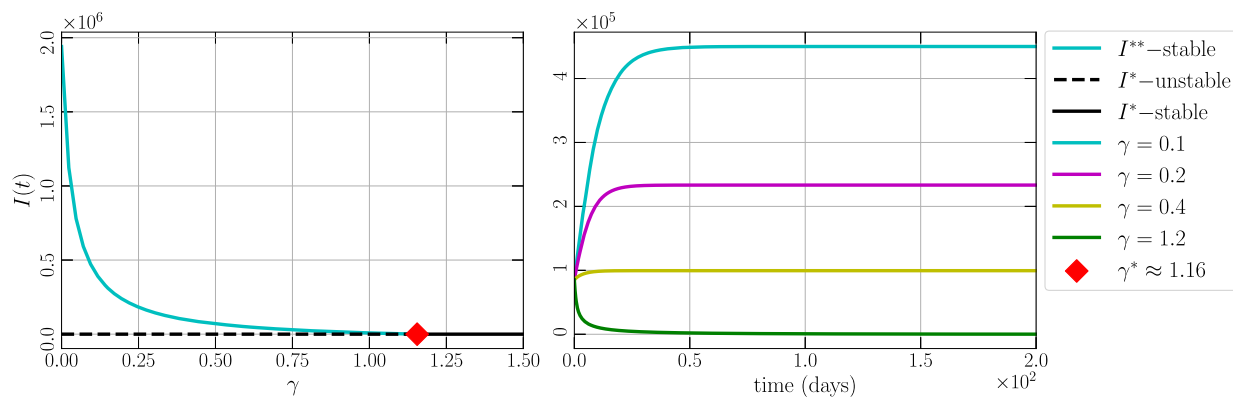
Fig. 10 Bifurcation diagram driven by γ and time-series of model (1) respect to $I(t)$

5.3 Bifurcations and dynamical behaviors

Based on PRCC results given in Table 3, we explore more the dynamical behaviors of model (1) by observing the change of the densities for each class when given parameters are varied. We first investigate the dynamical behaviors of model (1) when the second dose of vaccine rate (σ_1) is varied. As a result, we have numerical simulations given in Figs. 7 and 8. The density of people who received the first and second dose

of the MMR vaccine ($V_1(t)$ and $V_2(t)$), respectively, decrease and increase when σ_1 is increased which confirms the PRCC results given in Table 3. We also show that bifurcation does not exists for interval $0.7 \leq \sigma_1 \leq 1$. Furthermore, we investigate the impact of the effective contact rate (α) on the density of exposed class ($E(t)$) by portraying the bifurcation diagram along with its time-series with respect to $E(t)$ in Fig. 9 is the occurrence of forward bifurcation when α crosses the bifurcation point $\alpha^* \approx 3.9 \times 10^{-6}$. It is easy to compute that the
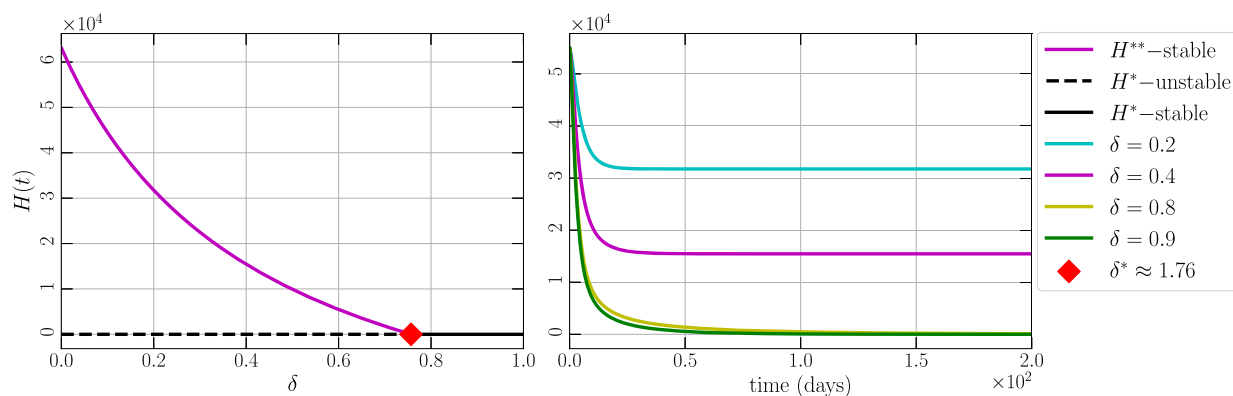
Fig. 11 Bifurcation diagram driven by δ and time-series of model (1) respect to $H(t)$
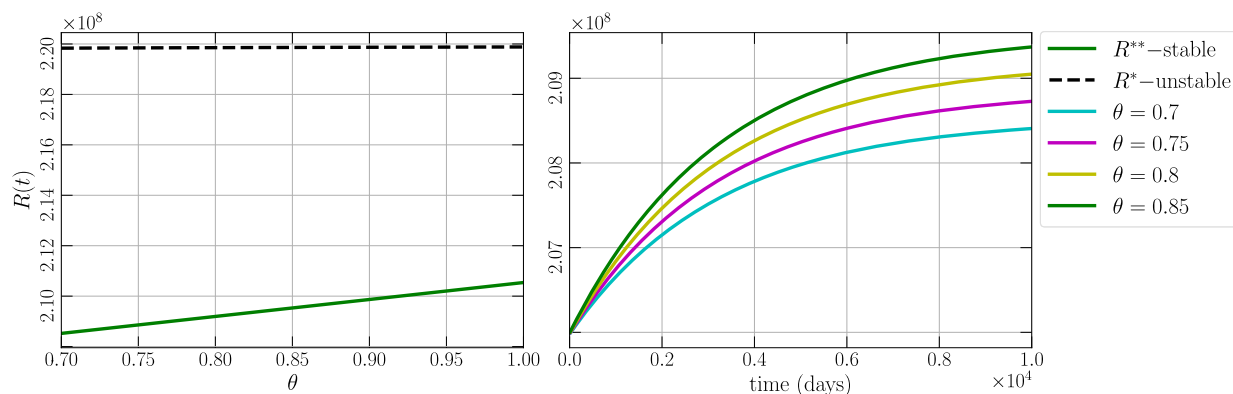
Fig. 12 Bifurcation diagram driven by θ and time-series of model (1) respect to $R(t)$

value of α^* is equal to $\mathcal{R}_0 = 1$. When $\alpha < \alpha^*$ or $\mathcal{R}_0 < 1$. The endemic point does not exist and the disease-free point becomes asymptotically stable. When α crosses α^* or $\mathcal{R}_0$ crosses 1, the disease-free point losses its stability while the asymptotically stable endemic point occurs in the interior via forward bifurcation. This also confirms that α has positive relationship with $E(t)$. Now, the dynamics of infected class ($I(t)$) are observed. The PRCC results show that they have negative relationship. This condition is confirmed by numerical simulations given in Fig. 10. The density of infected class ($I(t)$) decreases when γ increases and finally disappears when γ crosses $\gamma^* \approx 1.16$ This condition also shows the existence of forward bifurcation driven by γ where the bifurcation point is γ^* which equal to $\mathcal{R}_0 = 1$. Next, the influence of the measles death rate (δ) on the density of hospitalized class ($H(t)$) is observed. Again, the endemic point disappears via forward bifurcation where the bifurcation point at $R_0 = 1$ lies on $\delta^* = 1.76$, see Fig. 11). The density of $H(t)$ decreases as δ goes up. Finally, Fig. 12 is given to show the positive relationship between first dose of vaccine rate θ with recovered class ($R(t)$) given by the PRCC result in Fig. 6. When θ increases, $R(t)$ increases, which means that increasing the number of people who receive the first dose

of vaccine will save more life indicated by the increase in recovered people.

6 Conclusion

A mathematical model with seven compartments has been used to study the dynamics of the measles. The basic reproduction number is determined, and the boundary of solutions established. Two equilibrium points are identified, together with their stability results. To identify the most influential parameter on the threshold quantities, we performed a global sensitivity analysis by using the Partial Rank Correlation Coefficient (PRCC). The result from this analysis informs us of the most impactful parameter that contribute most to the spread and control of the disease. This parameter is the effective transmission rate α. We can say that restricting the interaction between susceptible and infected classes play the important role in reducing the growth rate of exposed and infected classes. The analysis further revealed that the most influential parameter for individuals who received the first and second dose of the MMR vaccine is the second dose of vaccine rate σ_1. Furthermore, the effect of the first and second

vaccine dose rates was demonstrated. Increasing vaccination rates reduces the number of infected people. An increase in the second dose vaccination rate in particular, has been shown to slow the spread of measles and suppress the endemic condition. The relevance of vaccination in containing and halting the spread of the measles has also been analyzed in this study. The most effective method of containing a measles outbreak in a population is vaccination. This finding suggests that the measles outbreak is reduced when vaccination rates increase. Therefore, mass vaccination campaigns should be encouraged to vaccinate the majority of the population in order to achieve a high level of herd immunity to the disease and stop a measles outbreak. In order to address vaccination gaps and stop measles outbreaks, government and public health officials may find it helpful to use the study's findings to develop strategic vaccination plans.

Declarations

Conflict of interest There are no conflicts of interest to declare.

Code Availability The code that support the findings of this study are available from the corresponding author upon reasonable request.

References

1. World Health Organization (2018) Measles. http://www.who.int/news-room/fact-sheets/detail/measles
2. Aldila D, Asrianti D (2019) A deterministic model of measles with imperfect vaccination and quarantine intervention. In: Journal of physics: conference series, vol 1218. IOP Publishing, p 012044
3. Dales L, Kizer KW, Rutherford G, Pertowski C, Waterman S, Woodford G (1993) Measles epidemic from failure to immunize. West J Med 159(4):455
4. World Health Organization (2019) Measles. https://www.who.int/news/item/15-05-2019-new-measles-surveillance-data-for-2019
5. Kuddus MA, Mohiuddin M, Rahman A (2021) Mathematical analysis of a measles transmission dynamics model in Bangladesh with double dose vaccination. Sci Rep 11(1):1–16
6. Nigeria Centre for Disease Control (2019) Measles. https://ncdc.gov.ng/diseases/info/m
7. Tilahun GT, Demie S, Eyob A (2020) Stochastic model of measles transmission dynamics with double dose vaccination. Infect Dis Model 5:478–494
8. Centre for Disease Control and Prevention (2019) Measles. https://www.cdc.gov/measles/symptoms/complications.html
9. Markowitz LE, Tomasi A, Sirotkin BI, Carr RW, Davis RM, Preblud SR, Orenstein WA (1987) Measles hospitalizations, united

states, 1977–84: comparison with national surveillance data. Am J Public Health 77(7):866–868
10. Lee B, Ying M, Stevenson J, Seward JF, Hutchins SS (2004) Measles hospitalizations, United States, 1985–2002. J Infect Dis 189(1Supplement–):S210–S215
11. Peter OJ, Viriyapong R, Oguntolu FA, Yosyingyong P, Edogbanya HO, Ajisope MO (2020) Stability and optimal control analysis of an SCIR epidemic model. J Math Comput Sci 10(6):2722–2753
12. Peter OJ, Kumar S, Kumari N, Oguntolu FA, Oshinubi K, Musa R (2022) Transmission dynamics of Monkeypox virus: a mathematical modelling approach. Model Earth Syst Environ. 8:3423–3434. https://doi.org/10.1007/s40808-021-01313-2
13. Peter OJ, Qureshi S, Yusuf A, Al-Shomrani M, Idowu AA (2021) A new mathematical model of Covid-19 using real data from Pakistan. Results Phys 24:104098
14. Peter OJ, Yusuf A, Oshinubi K, Oguntolu FA, Lawal JO, Abioye AI, Ayoola TA (2021) Fractional order of pneumococcal pneumonia infection model with Caputo Fabrizio operator. Results Phys 29:104581
15. Peter OJ (2020) Transmission dynamics of fractional order brucellosis model using caputo-fabrizio operator. Int J Differ Equ. https://doi.org/10.1155/2020/2791380
16. Abioye A, Ibrahim M, Peter O, Amadiegwu S, Oguntolu F (2018) Differential transform method for solving mathematical model of SEIR and SEI spread of malaria. Int J Sci Basic Appl Res 40(1):197–219
17. Abioye AI, Peter OJ, Ogunseye HA, Oguntolu FA, Oshinubi K, Ibrahim AA, Khan I (2021) Mathematical model of Covid-19 in Nigeria with optimal control. Results Phys 28:104598
18. Ayoola TA, Edogbanya HO, Peter OJ, Oguntolu FA, Oshinubi K, Olaosebikan ML (2021) Modelling and optimal control analysis of typhoid fever. J Math Comput Sci 11(6):6666–6682
19. Peter O, Ibrahim M, Oguntolu F, Akinduko O, Akinyemi S (2018) Direct and indirect transmission dynamics of typhoid fever model by differential transform method. J Sci Technol Educ 6:167–177
20. Bakare E, Adekunle Y, Kadiri K (2012) Modelling and simulation of the dynamics of the transmission of measles. Int J Comput Trends Technol 3:174–178
21. Okyere-Siabouh S, Adetunde I (2013) Mathematical model for the study of measles in cape coast metropolis. Int J Mod Biol Med 4(2):110–133
22. Tessa OM (2006) Mathematical model for control of measles by vaccination. Proc Mali Symp Appl Sci 2006:31–36
23. Huang J, Ruan S, Wu X, Zhou X (2018) Seasonal transmission dynamics of measles in China. Theory Biosci 137(2):185–195
24. Momoh A, Ibrahim M, Uwanta I, Manga S (2013) Mathematical model for control of measles epidemiology. Int J Pure Appl Math 87(5):707–717
25. Musyoki E, Ndungu R, Osman S (2019) A mathematical model for the transmission of measles with passive immunity. Int J Res Math Stat Sci 6(2):1–8
26. Ogunmiloro OM, Idowu AS, Ogunlade TO, Akindutire RO (2021) On the mathematical modeling of measles disease dynamics with encephalitis and relapse under the Atangana–Baleanu–Caputo fractional operator and real measles data of Nigeria. Int J Appl Comput Math 7(5):1–20
27. Peter O, Afolabi O, Victor A, Akpan C, Oguntolu F (2018) Mathematical model for the control of measles. J Appl Sci Environ Manag 22(4):571–576
28. Qureshi S et al (2020) Monotonically decreasing behavior of measles epidemic well captured by Atangana–Baleanu–Caputo fractional operator under real measles data of Pakistan. Chaos Solitons Fractals 131:109478
29. Ashraf F, Ahmad M (2019) Nonstandard finite difference scheme for control of measles epidemiology. Int J Adv Appl Sci 6(3):79–85

30. System BRFS et al (2017) Centers for disease control and prevention. https://www.cdc.gov/brfss/annual_data/annual_2016.html. Published 6 Dec 2017. Accessed 21 May

31. Diekmann O, Heesterbeek JAP, Metz JA (1990) On the definition and the computation of the basic reproduction ratio r 0 in models for infectious diseases in heterogeneous populations. J Math Biol 28(4):365–382

32. Steele J (2004) An introduction to the art of mathematical inequalities. The Cauchy–Schwarz master class MAA problem books series. Mathematical Association of America, Washington, DC

33. LaSalle J (1976) The stability of dynamical systems, regional conference series in applied mathematics. SIAM, Philadelphia, Khalid Hattaf Department of Mathematics and Computer Science. Hassan II University, PO Box, Faculty of Sciences Ben M'sik, p 7955

34. James Peter O, Ojo MM, Viriyapong R, Abiodun Oguntolu F (2022) Mathematical model of measles transmission dynamics using real data from Nigeria. J Differ Equ Appl. https://doi.org/10.1080/10236198.2022.2079411

35. Marino S, Hogue IB, Ray CJ, Kirschner DE (2008) A methodology for performing global uncertainty and sensitivity analysis in systems biology. J Theor Biol 254(1):178–196. https://doi.org/10.1016/j.jtbi.2008.04.011

36. Saltelli A (2002) Making best use of model evaluations to compute sensitivity indices. Comput Phys Commun 145(2):280–297. https://doi.org/10.1016/S0010-4655(02)00280-1

37. Saltelli A, Annoni P, Azzini I, Campolongo F, Ratto M, Tarantola S (2010) Variance based sensitivity analysis of model output. Design and estimator for the total sensitivity index. Comput Phys Commun 181(2):259–270. https://doi.org/10.1016/j.cpc.2009.09.018

Ⓐ Springer

Terms and Conditions